PPARγ accelerates cellular senescence by inducing p16^{INK4α} expression in human diploid fibroblasts

Qini Gan[1], Jing Huang[1], Rui Zhou[1], Jing Niu[1], Xiaojun Zhu[2], Jing Wang[1], Zongyu Zhang[1] and Tanjun Tong[1,*]

[1]Research Center on Aging, Department of Biochemistry and Molecular Biology, and [2]Cardiovascular Research Institute, Peking University Health Science Center, 38 Xueyuan Road, Beijing 100083, People's Republic of China

*Author for correspondence (e-mail: ttj@bjmu.edu.cn)

Accepted 14 April 2008
Journal of Cell Science 121, 2235-2245 Published by The Company of Biologists 2008
doi:10.1242/jcs.026633

Summary

Peroxisome proliferator-activated receptor γ (PPARγ) plays an important role in the inhibition of cell growth by promoting cell-cycle arrest, and PPARγ activation induces the expression of p16^{INK4α} (CDKN2A), an important cell-cycle inhibitor that can induce senescence. However, the role of PPARγ in cellular senescence is unknown. Here, we show that PPARγ promotes cellular senescence by inducing p16^{INK4α} expression. We found several indications that PPARγ accelerates cellular senescence, including enhanced senescence-associated (SA)-β-galactosidase staining, increased G1 arrest and delayed cell growth in human fibroblasts. Western blotting studies demonstrated that PPARγ activation can upregulate the expression of p16^{INK4α}. PPARγ can bind to the *p16* promoter and induce its transcription, and, after treatment with a selective PPARγ agonist, we observed more-robust expression of p16^{INK4α} in senescent cells than in young cells. In addition, our data indicate that phosphorylation of PPARγ decreased with increased cell passage. Our results provide a possible molecular mechanism underlying the regulation of cellular senescence.

Supplementary material available online at
http://jcs.biologists.org/cgi/content/full/121/13/2235/DC1

Key words: PPARγ, p16^{INK4α}, Cellular senescence, Fibroblast

Introduction

Cellular senescence, also known as replicative senescence, is a process during which cells lose their proliferative potential after a limited number of population doublings (PDs). Senescence is accompanied by a specific set of changes in morphology and in gene expression. For example, senescence-associated β-galactosidase (SA-β-gal) activity appears, the cell cycle is irreversibly arrested at the G1 phase and expression of cyclin-dependent kinase inhibitor (CDKI) increases (Hayflick, 1965; Wong and Riabowol, 1996). In addition, CDK4 and CDK6 can be inhibited by p16^{INK4α} (CDKN2A), an important cell-cycle inhibitor that can induce senescence (Collins and Sedivy, 2003). The p16^{INK4α} protein is thought to be an important biomarker of aging in vivo (Krishnamurthy et al., 2004) because its accumulation can trigger the onset of cellular senescence (Duan et al., 2001).

Caloric restriction (CR) increases the lifespan of many organisms. Some studies indicate that SIRT1 might mediate the effects of CR by repressing peroxisome proliferator-activated receptor γ (PPARγ) activity (Picard et al., 2004). PPARγ is a member of the nuclear receptor superfamily of ligand-activated transcription factors. PPARγ plays an important role the induction of cellular differentiation and the inhibition of cell growth by promoting cell-cycle arrest (Chang and Szabo, 2000; Elstner et al., 1998; Kubota et al., 1998; Mueller et al., 1998; Sarraf et al., 1998; Tontonoz et al., 1997). Guan et al. reported that PPARγ activation induces the expression of p16^{INK4α} and is accompanied by G1 arrest (Guan et al., 1999). Gizard et al. also demonstrated that PPARα, another member of the receptor superfamily to which PPARγ belongs, can bind to the *p16* promoter and increase p16^{INK4α} expression (Gizard et al., 2005). These data suggest that PPARγ can accelerate cellular senescence by regulating p16^{INK4α} expression. However, a role for PPARγ in senescence and the mechanisms by which PPARγ regulates p16^{INK4α} remain poorly understood. In the present study, we demonstrate a role for PPARγ in cellular senescence. Moreover, we identify the molecular mechanisms by which PPARγ regulates the expression of p16. Our results indicate that PPARγ dephosphorylation might play an important role in cellular senescence.

Results

Sustained PPARγ overexpression induced premature senescence and irreversible cell-growth arrest

The senescent state of normal human diploid fibroblast cells is characterized by enlarged, flattened cells with prominent lipofuscin granules and irreversible growth arrest (Hayflick and Moorhead, 1961). To determine the effects of PPARγ expression on cellular senescence, young 2BS (PD25) and WI-38 (PD20) cells were transfected with the expression plasmids pcDNA3.1 and pcDNA-PPARγ (termed vector and PPARγ, respectively). After sustained selection with G418, the transformants were obtained. Western blot results (Fig. 1A) confirmed that PPARγ overexpression significantly increased the expression of the wild-type PPARγ in 2BS and WI-38 cells. The transformants were analyzed for the relative senescence markers. Untransfected young, middle-aged and senescent 2BS cells were also analyzed for comparison (see supplementary material Fig. S1). To further analyze the effect of PPARγ activation on senescence, the influence of the selective PPARγ agonists troglitazone (20 μM) and pioglitazone (10 μM) (see supplementary material Fig. S1), which have reduced activity towards PPARα or PPARβ (Willson et al., 1996), on senescence markers was also tested.

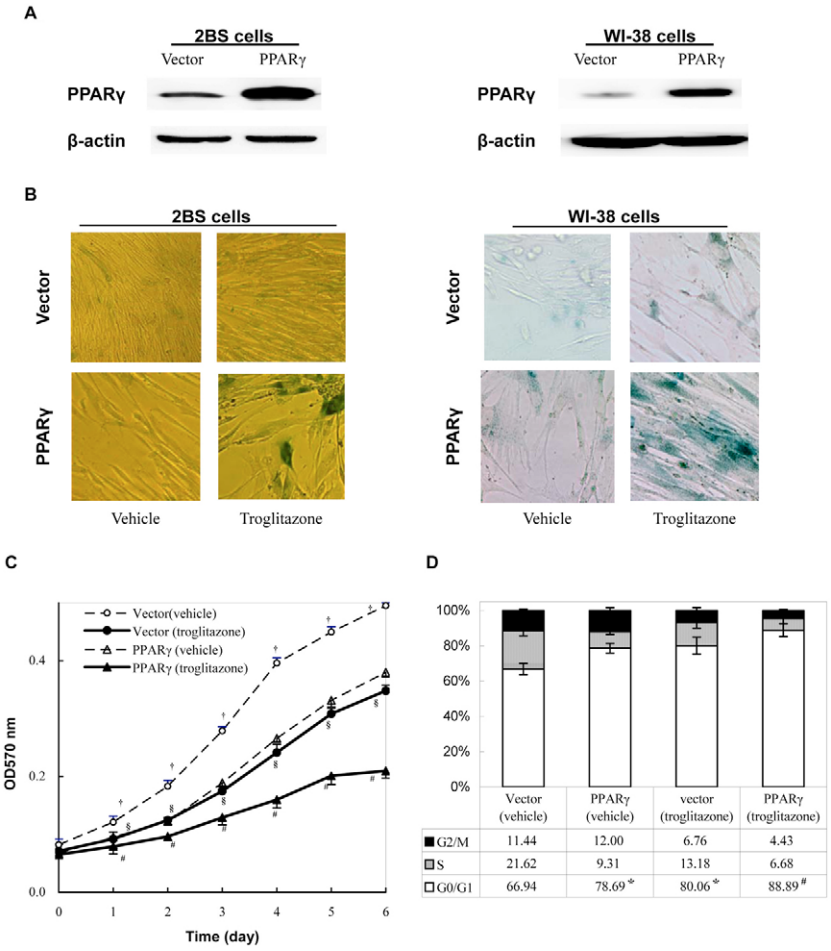

Fig. 1. Ligand-activated PPARγ induced changes associated with senescence and induced irreversible cell-growth arrest in 2BS and WI-38 cells. 2BS and WI-38 cells transfected with the expression plasmids pcDNA3.1 (vector) or pcDNA-PPARγ (PPARγ) were analyzed for the relative senescence markers (all transformants of 2BS cells at PD42 and WI-38 cells at PD37). Cells were treated with 20 μM troglitazone or DMSO (vehicle) as indicated. (A) Western blot analysis of PPARγ overexpression in PPARγ-transfected cells compared with vector-transfected cells. Western blotting was performed using specific antibodies against PPARγ as indicated. The β-actin lane serves as a loading control. (B) Vector-transfected and PPARγ-transfected cells were stained for SA-β-gal activity (blue), a classical marker of senescence. (C) Growth curves of vector-transfected and PPARγ-transfected cells were determined by the MTT assay. Values are the mean ± s.d. of triplicate points from a representative experiment (n=3), which was repeated three times with similar results. Values accompanied by different symbols are statistically significantly different from each other. (D) Flow-cytometry analysis of vector-transfected and PPARγ-transfected cells. Each experiment was performed at least three times. The table shows the representative data. The graph depicts data from three independent experiments (means ± s.d.). *P≤0.05 vs vehicle-treated vector cells; #P≤0.001 vs vehicle-treated vector cells.

PPARγ activation causes a senescence-like cell morphology and increased SA-β-gal activity

The specific senescence-associated marker pH 6.0 optimum β-galactosidase (SA-β-gal) was assayed by X-gal staining. Virtually all treated PPARγ cells (PD42) were strongly stained blue, with gross enlargement and flattened morphology resembling senescent cells (see supplementary material Fig. S1A). However, no significant morphological changes were observed in untreated vectors (PD42), which retained a refractive cytoplasm with long thin projections, and only a few dispersed cells were SA-β-gal-stained (Fig. 1B). For untreated PPARγ and treated vector cells (all at PD42), the positive ratio was comparable with that of middle-aged cells (PD42) (see Fig. 1B and supplementary material Fig. S1A). To determine whether the effect of PPARγ is a general accompaniment to senescence, we extended our study to investigate other normal human diploid fibroblast WI-38 cells. We obtained similar results (Fig. 1B).

The activation of PPARγ leads to growth inhibition

To observe the impact of PPARγ on cell proliferation, the growth curves for vector and PPARγ cells (all at PD42) were compared. The curve of treated PPARγ cells approached that of senescent cells (PD62), showing near complete inhibition of growth (see Fig. 1C and supplementary material Fig. S1B). Untreated PPARγ and treated vector cells had almost the same growth rate or growth potential as middle-aged cells (PD42); by contrast, untreated vector cells had stronger growth potential than untreated PPARγ and treated vector cells (see Fig. 1C and supplementary material Fig. S1B).

PPARγ activation accelerated G1 cell-cycle arrest

To clarify the mechanisms underlying growth-rate inhibition, the cell-cycle profile was analyzed by flow cytometry. Each experiment was performed at least three times and representative data are shown in Fig. 1D. Flow-cytometry assay revealed that PPARγ overexpression or agonist treatment increased the proportion of 2BS cells in the G0-G1 phases (P<0.05 vs vehicle-treated vector cells), and the greatest increase was observed when cells were both transfected with PPARγ and treated with agonist (P<0.001 vs vehicle-treated vector cells) (see Fig. 1D and supplementary material Fig. S1C). Thus, PPARγ activation might influence cell proliferation by influencing cell-cycle progress.

PPARγ activation results in a reduction of the 2BS replicative lifespan

The replicative senescence of normal human diploid fibroblasts is directly correlated to the number of PDs rather than to the growth and metabolic time (Dai and Enders, 2000; Hayflick, 1965). After completing a finite number of divisions, cells enter permanent growth arrest. To determine the effects of PPARγ overexpression on the lifespan of 2BS cells, the number of PDs for PPARγ-transfected and vector-transfected cells from the same batch of young cells was counted. The results revealed that PPARγ cells treated with troglitazone ceased cell division approximately 12 PDs earlier than did vector cells treated with troglitazone. Notably, treated PPARγ cells ceased dividing 17 PDs earlier than did untreated vector cells and 19 PDs earlier than did normal cells. Untreated PPARγ and treated vector cells had a slightly shorter lifespan than did untreated vector cells (Table 1).

Silencing PPARγ delays a senescence-like state and induces lifespan extension

To determine the effects of PPARγ silencing on cellular senescence, young 2BS and WI-38 cells were transfected with the expression

Table 1. Cumulative population doublings of cells transfected with vector, PPARγ or control

Cells	Cumulative PDs (means ± s.e.)
Vector (vehicle)	61±1
Vector (troglitazone)	56±1
PPARγ (vehicle)	56±1
PPARγ (troglitazone)	44±2*
Untransfected	63±2

*$P \leq 0.05$ vs vehicle-treated vector-transfected cells.

plasmids pSilencer 2.1-U6 neo and pSilencer-PPARγ (termed RNAi vector and siPPARγ, respectively). After sustained drug selection, G418-resistant cell clones were obtained. Using western blotting, we detected the expression of PPARγ in vector-transfected and siPPARγ-transfected cells. We found that, in siPPARγ-transfected cells, PPARγ levels decreased significantly relative to RNAi-vector-transfected cells (Fig. 2A). Transfected cells were then analyzed for relative senescence markers.

PPARγ silencing inhibits SA-β-gal activity

No SA-β-gal activity was observed in treated and untreated siPPARγ cells (all at PD51), whereas treated RNAi-vector cells (PD51) were strongly stained blue. Only sporadic SA-β-gal-positive cells were observed in untreated RNAi vectors (PD51) (Fig. 2B). We obtained similar results with WI-38 cells (Fig. 2B).

siPPARγ promotes cell growth

The impact of PPARγ gene-specific silencing on cell growth was evaluated. The curve of treated and untreated siPPARγ cells (all at PD51) advanced quickly, indicative of a strong proliferation potential. Control-treated and untreated RNAi-vector cells (all at PD51) grew slower than did the siPPARγ cells. Moreover, untreated RNAi-vector cells grew slightly faster than did the treated RNAi-vector cells (Fig. 2C).

siPPARγ postponed G1 cell-cycle arrest

Treated and untreated siPPARγ cells (all at PD51) exhibited significantly postponed irreversible growth arrest, whereas treated and untreated RNAi-vector cells (all at PD51) exhibited an increased proportion of 2BS cells in the G0-G1 phases. Furthermore, treated RNAi-vector cells had a slightly higher percentage of cells in the G0-G1 phases than did the corresponding untreated RNAi-vector cells (Fig. 2D).

siPPARγ results in a finite extension of 2BS replicative lifespan

To determine the effects of PPARγ gene-specific silencing on the lifespan of 2BS cells, the number of PDs for siPPARγ-transfected and RNAi-vector-transfected cells from the same batch of young cells was counted. The lifespan of treated siPPARγ cells was about 17 PDs longer than treated RNAi-vector cells and about 13 PDs longer than untreated RNAi-vector cells. Treated RNAi-vector cells had a slightly shorter lifespan than did the untreated RNAi-vector cells. No significant lifespan extension was observed in untreated siPPARγ cells or treated siPPARγ cells (Table 2). Taken together, these findings indicated that PPARγ activation could weaken the replicative capacity, reduce the replicative lifespan, and ultimately promote the onset of senescence of 2BS and WI-38 cells, whereas RNAi-mediated silencing of PPARγ gene exerted the opposite effects.

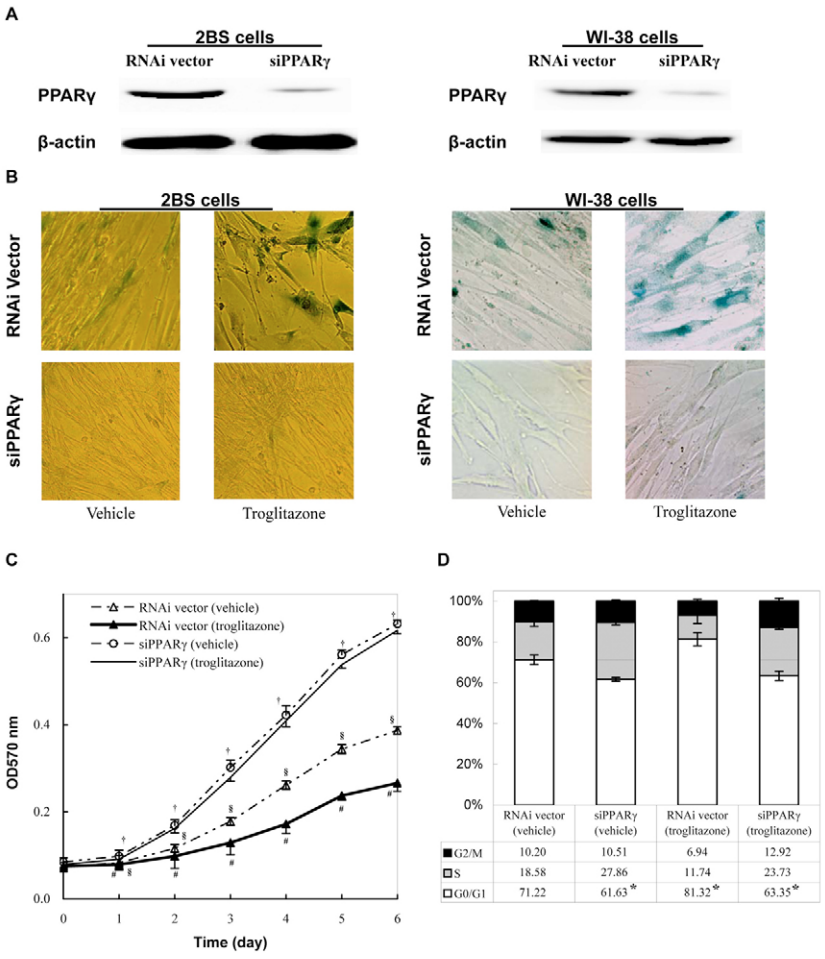

Fig. 2. The silencing of PPARγ suppressed the senescence-associated features and cell proliferation in 2BS and WI-38 cells. 2BS and WI-38 cells transfected with the expression plasmids pSilencer 2.1-U6 neo (RNAi vector) or pSilencer-PPARγ (siPPARγ) were analyzed for the relative senescence markers (all transformants of 2BS at PD51 and WI-38 at PD47). Cells were treated with 20 μM troglitazone or DMSO (vehicle) as indicated. (A) Western blot analysis of PPARγ silencing in siPPARγ-transfected cells compared with RNAi-vector-transfected cells. Western blotting was performed using specific antibodies against PPARγ as indicated. The β-actin lane serves as a loading control. (B) RNAi-vector-transfected and siPPARγ-transfected cells were stained for SA-β-gal activity (blue), a classical marker of senescence. (C) Growth curves of RNAi-vector-transfected and siPPARγ-transfected 2BS cells were determined by the MTT assay. Values are the mean ± s.d. of triplicate points from a representative experiment (n=3), which was repeated three times with similar results. Values accompanied by different symbols are statistically significantly different from each other. (D) Flow-cytometry analysis of RNAi-vector-transfected and siPPARγ-transfected 2BS cells. Each experiment was performed at least three times. The table shows the representative data. The graph depicts data from three independent experiments (means ± s.d.). *$P \leq 0.05$ vs vehicle-treated RNAi-vector cells.

Table 2. Cumulative population doublings of cells transfected with RNAi vector or siPPARγ

Cells	Cumulative PDs (means ± s.e.)
RNAi vector (vehicle)	59±1
RNAi vector (troglitazone)	55±1
siPPARγ (vehicle)	73±1*
siPPARγ (troglitazone)	72±1*

*$P \leq 0.05$ vs vehicle-treated RNAi-vector-transfected cells.

PPARγ-mediated regulation of p16^{INK4α} expression

Previous work reported that PPARγ activation induces the expression of p16^{INK4α} (Guan et al., 1999) and that accumulation of p16^{INK4α} triggers the onset of cellular senescence (Duan et al., 2001). Therefore, we hypothesized that *p16* is a PPARγ target gene. First, we determined whether PPARγ overexpression could upregulate p16 protein expression. Western blot analysis revealed that PPARγ overexpression or troglitazone treatment enhanced p16 protein levels in 2BS and WI-38 cells, and the greatest increase was observed when cells were both overexpressed with PPARγ and treated with troglitazone (Fig. 3A). To further verify this finding, we silenced the PPARγ gene and examined the p16^{INK4α} protein levels in 2BS and WI-38 cells. Western blot assays revealed markedly reduced p16^{INK4α} expression in the siPPARγ-transfected cells compared with RNAi-vector-transfected cells. Furthermore, PPARγ-agonist treatment did not increase p16^{INK4α} levels (Fig. 3B). To determine the specificity and efficiency of siPPARγ, we detected the expression of related proteins in RNAi-vector-transfected, negative-transfected [the expression plasmids pSilencer-negative control small interfering RNA (siRNA) with sequences that have no homology to any known mammalian gene, termed as negative] and siPPARγ-transfected cells by western blotting. Our findings show that, in siPPARγ-transfected cells, the PPARγ level reduced markedly compared with RNAi-vector- and negative-transfected cells. However, the levels of PPARα and PPARβ in siPPARγ-transfected cells were similar to RNAi-vector- and negative-transfected cells (see supplementary material Fig. S2A). These data identified the specificity and efficiency of siPPARγ. Western blot assays revealed a decreased p16^{INK4α} expression in siPPARγ-transfected cells compared with negative-transfected cells (see supplementary material Fig. S2B). The results were consistent with Fig. 3B, which confirmed further that the knockdown of PPARγ caused a reduction in p16^{INK4α} expression. These results suggest that PPARγ activation upregulates the expression of p16^{INK4α}.

PPARγ binds to the PPRE-containing region of the endogenous *p16* promoter

We examined in vivo DNA-binding activity of PPARγ to the *p16* promoter. A peroxisome proliferator response element (PPRE) has been identified in the *p16* promoter sequence (Fig. 4A) and is located at position –1023 relative to the translation initiation site (Gizard et al., 2005). We found that PPARγ bound the PPRE both in young cells and in senescent cells, and both young and senescent cells had similar amplification without troglitazone stimulation (Fig. 4B). However, the binding of PPARγ was more robust in senescent cells than in young cells after stimulation with troglitazone or pioglitazone (Fig. 4B,D). Real-time PCR can increase the accuracy and precision of chromatin immunoprecipitation (ChIP) measurements, allowing for the detection of changes of less than twofold (Johnson and Bresnick, 2002). Quantitative real-time PCR analyses revealed that,

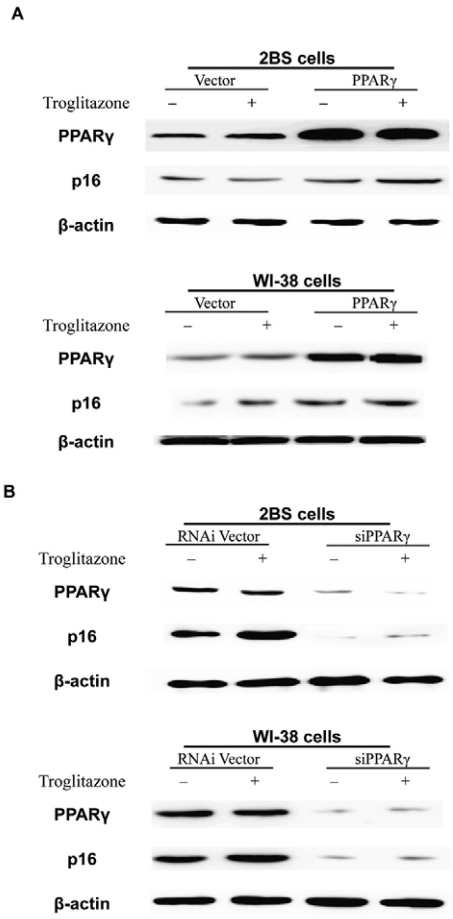

Fig. 3. PPARγ activation increases p16 protein levels in 2BS and WI-38 cells. 2BS and WI-38 cells were transfected with the expression plasmids pcDNA3.1 (vector), pcDNA3.1-PPARγ (PPARγ), pSilencer 2.1-U6 neo (RNAi vector) or pSilencer-PPARγ (siPPARγ) and treated, as indicated, with 20 μM troglitazone or DMSO (vehicle) for 72 hours. (A) Western blot analysis of PPARγ and p16^{INK4α} expression in vector-transfected or PPARγ-transfected cells. (B) Western blot analysis of PPARγ and p16^{INK4α} expression in RNAi-vector-transfected or siPPARγ-transfected cells. Western blotting was performed using specific antibodies against PPARγ and p16^{INK4α} as indicated. The β-actin lane served as a loading control.

after treatment with PPARγ agonists, there was a significant increase in the binding activity of PPARγ in both young and senescent 2BS cells, but the magnitude of change was much greater in senescent 2BS cells (Fig. 4C,E). Following the addition of GW9662, a PPARγ antagonist (Bendixen et al., 2001; Wright et al., 2000), the binding of PPARγ was weaker in senescent cells than in young cells (Fig. 4F). These results indicate that PPARγ binds to the *p16* promoter in vivo and imply that the role of PPARγ in *p16* transcriptional regulation is ligand dependent. As negative controls, PCR amplification using primers covering a region located immediately downstream of the –1023 site (PPRE) failed to yield a significant signal (Fig. 4G); neither the irrelevant antibody control (β-actin) nor the negative control (no antibody sample) had amplification products. Taken together, these results demonstrated the specificity of PPARγ immunoprecipitation and PCR amplification.

Ligand-activated PPARγ induces transcription of *p16*

Subsequently, we analyzed the effects of PPARγ on the expression of the *p16* reporter gene, in which the luciferase gene is driven by

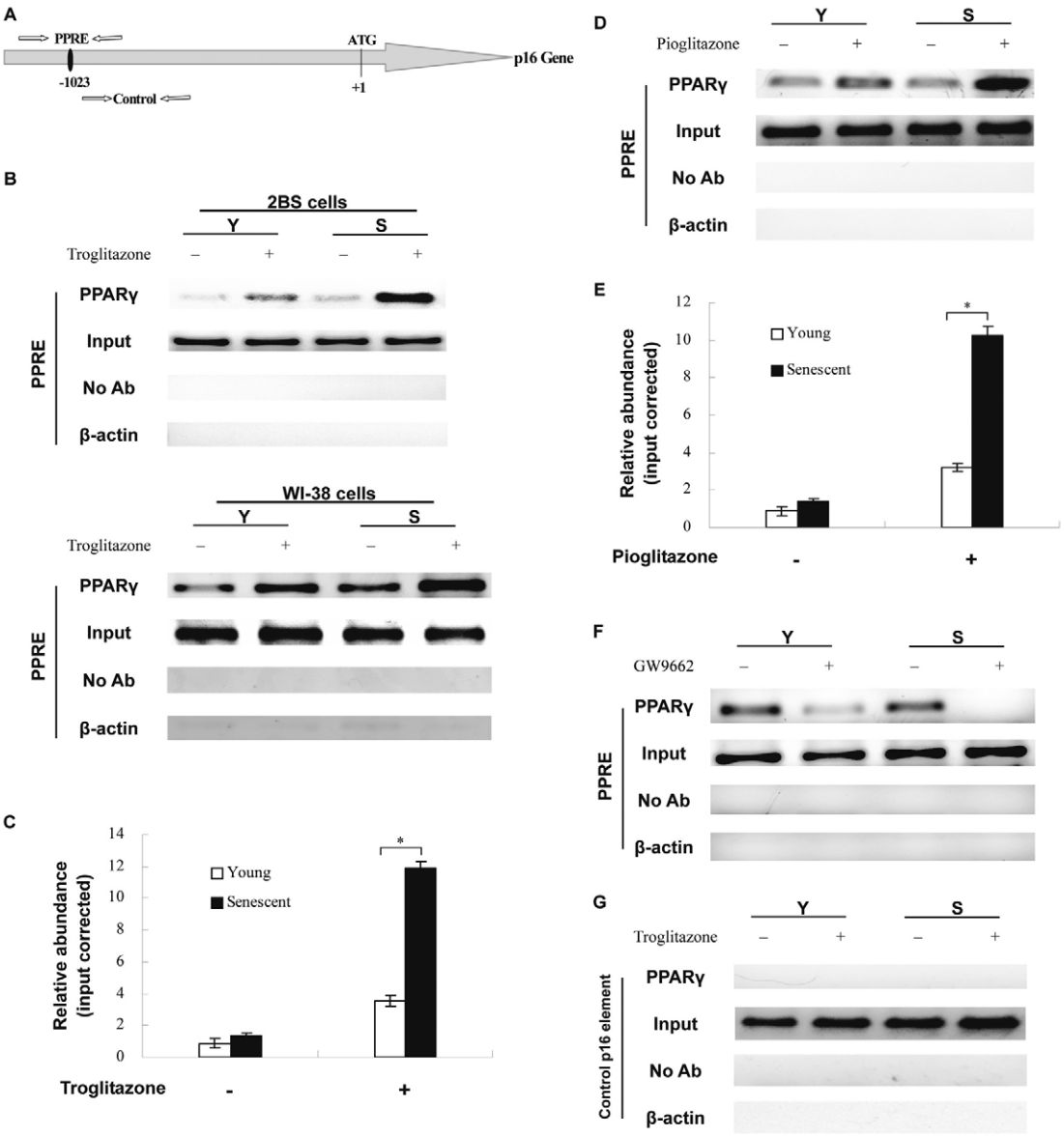

Fig. 4. PPARγ binds to the PPRE-containing region in the *p16* gene promoter. (A) Schematic diagram of the *p16* gene promoter. 'PPRE' denotes putative PPARγ-binding sites and 'control' denotes a region located immediately downstream of PPRE. The numbers are the positions upstream of the *p16* gene translation initiation site. (B) Soluble chromatin was prepared from 2BS cells [young (Y; PD25) or senescent (S; PD62)] or WI-38 cells [young (Y; PD20) or senescent (S; PD50)] treated (+) or not (–) with 20 μM troglitazone for 48 hours. (C-E) Soluble chromatin was prepared from young or senescent 2BS cells treated or not with 20 μM troglitazone (C) or 10 μM pioglitazone (D,E) for 48 hours. Precipitated DNA samples were amplified with primers recognizing the PPRE domain. ChIP assays were quantified by real-time PCR (C,E). Values are expressed relative to the controls (untreated young 2BS cells), which were set as 1. Values are the mean ± s.d. of triplicate points from a representative experiment (n=3), which was repeated three times with similar results. *$P \leqslant 0.05$. (F) Soluble chromatin was prepared from young or senescent 2BS cells treated or not with 10 μM GW9662 for 48 hours. Precipitated DNA samples were amplified with primers recognizing the PPRE domain. (G) Soluble chromatin was prepared from young or senescent 2BS cells treated or not with 20 μM troglitazone for 48 hours. Precipitated DNA samples were amplified with primers recognizing the control element as indicated in A. IP was performed with an antibody against PPARγ and DNA was amplified using primer pairs as indicated. As negative controls, the no antibody (No Ab) sample is an immunoprecipitation that did not contain antibody, and antibody against β-actin was used as an irrelevant antibody control. The input sample (Input) contained 0.5% of the total starting chromatin. The ChIP assays were repeated three times, and results of a representative experiment are shown.

a *p16* promoter. 2BS cells were transfected with various combinations of plasmids that expressed pcDNA3.1, pcDNA-PPARγ, pSilencer 2.1-U6 neo or pSilencer-PPARγ together with wild-type and mutant p16-Luc (luciferase). Cells were then treated with troglitazone (20 μM), pioglitazone (10 μM) or GW9662 (10 μM). Reporter activity was enhanced by treatment with PPARγ agonists, and this activity was higher in cell lysates that contained PPARγ from senescent cells (about 13-fold) than in those that contained PPARγ from young cells (about fourfold) (Fig. 5A). In WI-38 cells, reporter activity was also higher in cell lysates that contained PPARγ from senescent cells (about tenfold) than in those that contained PPARγ from young cells (about sixfold) (Fig. 5A). Mutation of p16-Luc or siPPARγ resulted in a significant, albeit incomplete, reduction of *p16* promoter activation (Fig. 5A,B).

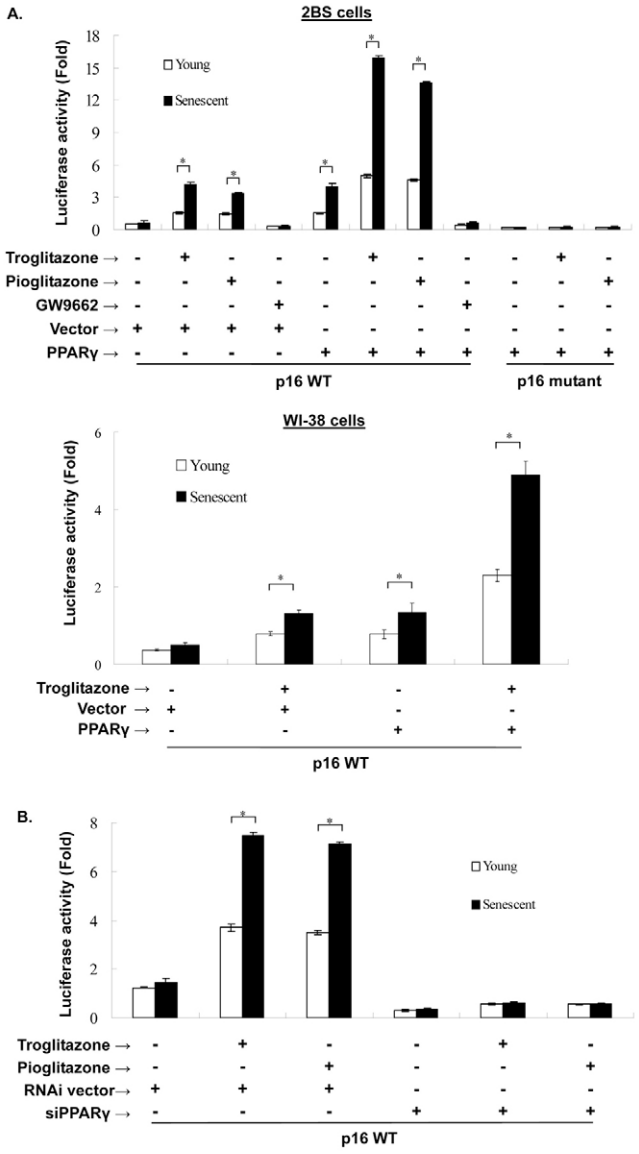

Fig. 5. Induction of human *p16* promoter activity by ligand-activated PPARγ. (A) 2BS and WI-38 cells were transfected with expression plasmids pcDNA3.1 (vector) or pcDNA-PPARγ (PPARγ) as indicated, together with wild-type p16-Luc (p16 WT) or mutant p16-Luc (p16 mutant). (B) 2BS cells were transfected with expression plasmids pSilencer 2.1-U6 neo (RNAi vector) or pSilencer-PPARγ (siPPARγ) as indicated, together with wild-type p16-Luc (p16 WT). Cells were subsequently treated with 20 μM troglitazone, 10 μM pioglitazone or 10 μM GW9662. Luciferase activities were then measured 24 hours after treatment. Values are the mean ± s.d. of triplicate points from a representative experiment (n=3), which was repeated three times with similar results. *P≤0.05.

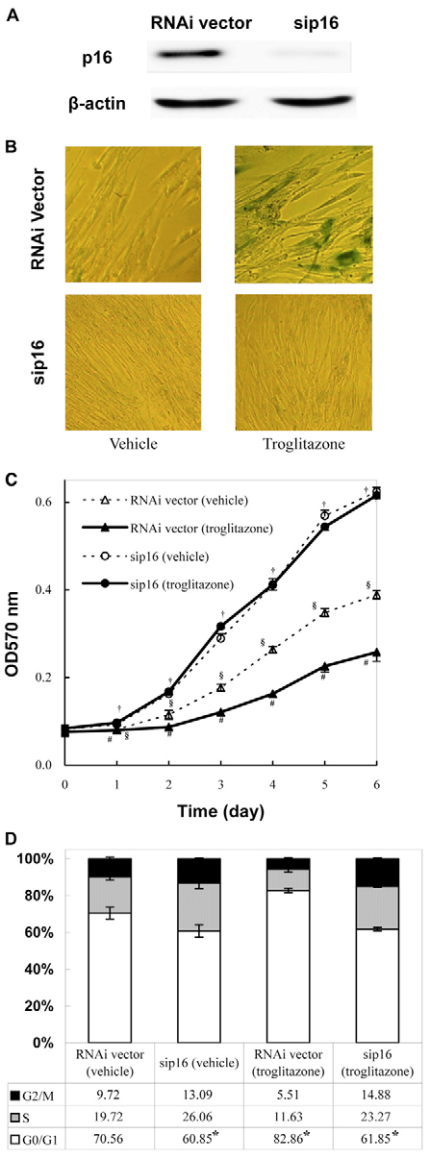

Fig. 6. The silencing of p16 in 2BS cells prevented the appearance of senescence-associated features and the growth-inhibition effects of PPARγ agonists. 2BS cells transfected with the expression plasmids pSilencer 2.1-U6 neo (RNAi vector) or pSilencer-p16 (sip16) were analyzed for the relative senescence markers (all at PD51). Cells were treated with 20 μM troglitazone or DMSO (vehicle) as indicated. (A) Western blot analysis of p16 silencing in sip16-transfected cells compared with RNAi-vector-transfected cells. Western blotting was performed using specific antibodies against $p16^{INK4\alpha}$ as indicated. The β-actin lane serves as a loading control. (B) RNAi-vector-transfected and sip16-transfected cells were stained for SA-β-gal activity (blue), a classical marker of senescence. (C) Growth curves of RNAi-vector-transfected and sip16-transfected 2BS cells were determined by the MTT assay. Values are the mean ± s.d. of triplicate points from a representative experiment (n=3), which was repeated three times with similar results. Values accompanied by different symbols are statistically significantly different from each other. (D) Flow-cytometry analysis of RNAi-vector-transfected and sip16-transfected 2BS cells. Each experiment was performed at least three times. The table shows the representative data. The graph depicts data from three independent experiments (means ± s.d.). *P≤0.05 vs vehicle-treated RNAi-vector cells.

Identical results were obtained in cells treated with GW9662 (10 μM) (Fig. 5A). Taken together, these data suggest that ligand-activated PPARγ induced transcriptional activity of the *p16* promoter, and this induction was stronger in senescent cells than in young cells.

Silencing the *p16* gene by RNA interference

In order to further verify that PPARγ could promote senescence via $p16^{INK4\alpha}$, we evaluated the role of p16 in mediating the senescence effects of PPARγ activation in 2BS cells. Young 2BS cells (PD25) were transfected with the expression plasmids pSilencer 2.1-U6 neo and pSilencer-p16 (termed RNAi vector and sip16, respectively). After sustained selection with G418, the transformants (all at PD51)

were obtained. Western blot results revealed that, in sip16-transfected cells, p16 levels decreased significantly relative to RNAi-vector-transfected cells (Fig. 6A). It is noteworthy that, similar to what occurred in siPPARγ-transfected cells, the SA-β-gal-positive staining ratio was drastically decreased in treated and untreated sip16-transfected cells (Fig. 6B, Fig. 2B). Interestingly, sip16-transfected cells proliferated at a much higher rate than did RNAi-vector-transfected cells. Moreover, sip16-transfected cells did not respond to troglitazone treatment (Fig. 6C). Accordingly, the ratios of cells in G0-G1 phases were reduced in sip16-transfected cells and were not affected by troglitazone treatment (Fig. 6D). Altogether, these data indicate that the silencing of $p16^{INK4\alpha}$ caused resistance to PPARγ-agonist-induced senescence.

PPARγ expression in young and senescent cells

Because PPARγ DNA-binding activity and transcriptional activity increased as cells approached the end of their replicative lifespan in culture, we further evaluated the expression patterns of PPARγ during successive passages. We therefore measured endogenous mRNA and protein expression levels of PPARγ and $p16^{INK4\alpha}$. Using reverse transcription-polymerase chain reaction (RT-PCR), *PPARγ* mRNA, *p16* mRNA and *GAPDH* mRNA levels were analyzed in young (PD25), middle-aged (PD42) and senescent (PD62) 2BS cells. Our findings demonstrate that the levels of *PPARγ* mRNA were similar in young, middle-aged and senescent cells, whereas the *p16* mRNA levels were increased in senescent cells relative to other groups (Fig. 7A). In addition, western blot analysis was performed on the 2BS and WI-38 cells. Protein levels of PPARγ did not change appreciably as cells aged, whereas $p16^{INK4\alpha}$ protein levels increased as cells aged in culture (Fig. 7B).

Phosphorylation of PPARγ represses its transactivating function

The above findings indicate that PPARγ levels remain constant in young and senescent cells, but they do not explain why the transcriptional activity of PPARγ increased in senescent cells. Phosphorylation modifications reportedly affect PPARγ transcriptional activity (Hu et al., 1996; Lazennec et al., 2000; Han et al., 2000); therefore, we analyzed the phosphorylation state of PPARγ in young and senescent 2BS and WI-38 cells. We found that the phosphorylation level of PPARγ decreased as cells aged (Fig. 8A). To evaluate the effect of PPARγ phosphorylation on its transcriptional function, we created a mutant of pcDNA-PPARγ, in which the serine at position 84, the potential phosphorylation site, was changed to alanine [pcDNA-PPARγ (S84A)]. We then analyzed the effects of PPARγ phosphorylation on the expression of the *p16* reporter gene in which the luciferase gene is driven by the *p16* promoter. 2BS cells were transfected with various combinations of plasmids that expressed pcDNA3.1(–), pcDNA-PPARγ (WT) or mutant pcDNA-PPARγ(S84A) together with wild-type p16-Luc. Cells were then treated with troglitazone (20 μM) or pioglitazone (10 μM). The results revealed that the untreated mutant PPARγ (S84A) exhibited greater transactivation (about 4.5-fold) than untreated wild-type PPARγ (about twofold). Furthermore, the treated S84A mutant activated luciferase expression to a significantly greater extent (about 6.5-fold) than treated wild-type PPARγ (about threefold). Our finding indicated that the S84A mutant showed a high level of transactivation, comparable with that of wild-type PPARγ (Fig. 8B). Taken together, these data suggest that phosphorylation of PPARγ represses its transcriptional activity.

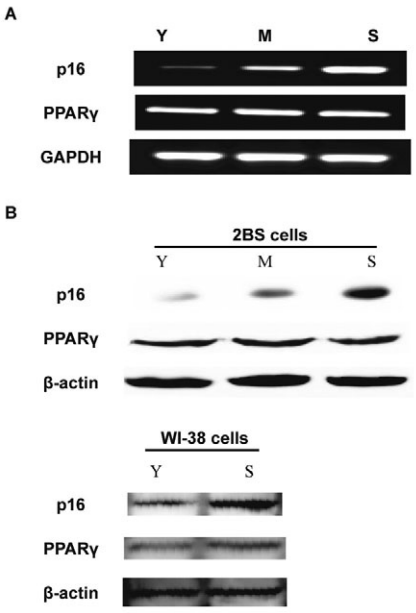

Fig. 7. The expression level of PPARγ. (A) The relative amounts of *p16*, *PPARγ* and *GAPDH* mRNA in young (Y; PD25), middle-aged (M; PD42) and senescent (S; PD62) 2BS cells. Total RNA was isolated as indicated and then subjected to RT-PCR analysis using PPARγ or p16 primers. GAPDH was used as an internal control for normalization purposes. (B) Western blot analysis of PPARγ and $p16^{INK4\alpha}$ expression in 2BS and WI-38 cells. Total proteins were extracted, and western blotting was performed using specific antibodies against PPARγ and $p16^{INK4\alpha}$ as indicated. The β-actin lane serves as a loading control.

Discussion

Senescence is the state or process of aging at the cellular level, and is thought to relate to age-related diseases and tumorigenesis (Campisi, 2001; Campisi, 2005; Weinstein and Ciszek, 2002). Senescence may be described as accumulated DNA damage, a limited number of cell divisions and a decreased ability to remove free radicals (Weinstein and Ciszek, 2002). CR has been proposed to extend lifespan and slow aging. Some studies suggest that SIRT1, the primary molecule mediating the effects of CR, functions by repressing PPARγ activity (Picard et al., 2004). PPARγ might play an important role in cellular senescence; however, the function of PPARγ in the progression of cellular senescence has never been described. In the present study, we demonstrated that PPARγ activation promoted cellular senescence (Figs 1, 2), an effect attributed to the induction of p16. $p16^{INK4\alpha}$ is an important cell-cycle inhibitor, and its accumulation triggers the onset of cellular senescence (Duan et al., 2001). An upregulation of $p16^{INK4\alpha}$ expression by PPARγ agonists provides a mechanism for senescence being repressed by CR and also a model (Fig. 9) that regulates cellular senescence.

The nuclear receptor superfamily of PPARs regulates the transcription of numerous target genes after dimerizing with the retinoid X receptor (RXR) and binding to PPRE (a specific DNA-binding site) (Mangelsdorf et al., 1995). PPREs usually consist of a direct repeat of the hexanucleotide AGGTCA sequence, separated by one or two nucleotides (DR1 or DR2) (Michalik et al., 2004). Recently, one report indicated that PPARα can bind to PPRE in the *p16* promoter and increase $p16^{INK4\alpha}$ expression (Gizard et al., 2005). Because the nuclear receptor superfamily of PPARs can bind to the same DNA-binding site, PPRE, we hypothesize that PPARγ can

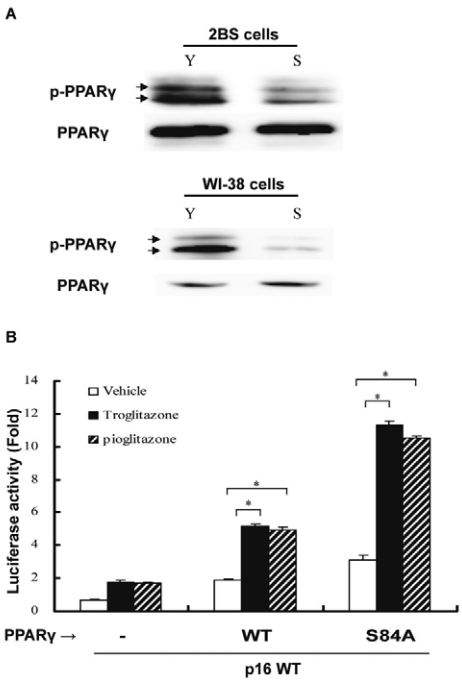

Fig. 8. Phosphorylation represses the transactivating function of PPARγ. (A) Western blot analysis of phosphorylation levels of PPARγ in young and senescent 2BS and WI-38 cells. Total proteins were extracted, and western blotting was performed using specific antibodies against PPARγ and phosphorylated PPARγ (p-PPARγ) as indicated. Arrow indicates phosphorylated PPARγ, and the observed doublet is reported as two translation initiation sites. (B) 2BS cells were transfected with expression plasmids pcDNA3.1 (–), pcDNA-PPARγ (WT) or mutant pcDNA-PPARγ(S84A) as indicated, together with wild-type p16-Luc. Cells were subsequently treated with 20 μM troglitazone or 10 μM pioglitazone. Luciferase activities were measured 24 hours after treatment. Values are the mean ± s.d. of triplicate points from a representative experiment (n=3), which was repeated three times with similar results. *$P \leqslant 0.05$.

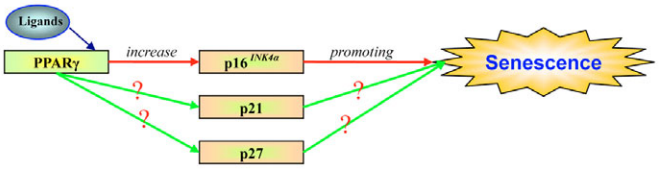

Fig. 9. Model of PPARγ-regulated cellular senescence.

also bind to PPRE in the *p16* promoter and thereby regulate $p16^{INK4\alpha}$ expression. Western blot analysis demonstrated that PPARγ overexpression and PPARγ-agonists treatment enhanced endogenous expression of $p16^{INK4\alpha}$, whereas RNA interference of PPARγ inhibited the expression of $p16^{INK4\alpha}$ (Fig. 3). These results suggested that the activation of PPARγ induced the expression of $p16^{INK4\alpha}$ in 2BS and WI-38 cells.

In the search for the molecular mechanisms involved in the regulation by PPARγ of *p16*, PPARγ activation was found to upregulate *p16* promoter activity, thus identifying for the first time a molecular mechanism by which PPARγ directly interferes with senescence progression. We observed that both DNA-binding activity and transcriptional activity of PPARγ were increased several fold in senescent cells, and the increased activity is ligand-dependent (Figs 4, 5).

2BS cells were previously isolated from human fetal lung fibroblast tissue and have been fully characterized (Tang et al., 1994). The maximum population doubling of human diploid fibroblasts is limited in culture, so they are widely used as a model of cellular senescence. Previous reports have suggested that fibroblast cellular senescence occurs as a consequence of a 'genetic program' (Goldstein, 1990). This program has been partially characterized by gene expression patterns during the progression of successive passages. Sasaki et al. reported that *PPARγ* mRNA levels do not significantly differ by sex or age in lung tissue (Sasaki et al., 2002). However, Ye et al. found that the expression of PPARγ at both the mRNA and protein level in adipose tissue of older rats was dramatically decreased and, likewise, that the expression of *PPARγ* mRNA in omental adipose tissue of elderly men was significantly decreased (Ye et al., 2006). These conflicting data regarding PPARγ expression patterns might be due to the various roles of PPARγ in different tissues during the progression of successive passages. Because PPARγ activation increases during aging, fat-deposit size reportedly declines and lipids are redistributed to muscle, bone marrow and other tissues (Moerman et al., 2004; Kirkland et al., 2002). Our results indicate that the mRNA and protein level of PPARγ in young cells is similar to that in senescent cells (Fig. 7). We found that PPARγ activity increased in senescent cells, although the expression of PPARγ did not appear to be upregulated.

Research has demonstrated that PPARγ activity is modulated by phosphorylation, which inhibits PPARγ transcriptional activity (Hu et al., 1996; Lazennec et al., 2000; Han et al., 2000). To determine why the transcriptional activity of PPARγ increases as cells age, we analyzed the phosphorylation state of PPARγ in both young and senescent 2BS and WI-38 cells. As expected, the levels of PPARγ phosphorylation decreased as cells aged (Fig. 8A). We also found that mutant PPARγ (mutation of serine 84 to alanine, which abolished phosphorylation of PPARγ) has higher transcriptional activity than wild-type PPARγ (Fig. 8B). These results indicate that phosphorylation of PPARγ represses the transcriptional activity of PPARγ itself. Three possible mechanisms may explain the modulation of PPARγ transactivation activity: (a) phosphorylation of PPARγ might decrease its affinity for its cognate ligand; (b) the phosphorylation of PPARγ could influence its interactions with co-repressors and/or coactivators of transcription; and (c) phosphorylation of PPARγ might promote its degradation by the ubiquitin-proteasome system in response to ligand activation. According to the first mechanism, hyperphosphorylated PPARγ should exhibit decreased ligand binding. Our results indicated that the DNA-binding activity and transcriptional activity of PPARγ increased upon agonist treatment and these changes were much greater in senescent cells than that in young cells (Figs 4, 5). This indicated that, in young cells, hyperphosphorylation of PPARγ decreases its transcriptional activity. However, hyperphosphorylation of PPARγ does not alter its DNA-binding activity, because the DNA-binding activity of PPARγ is similar in untreated young cells and untreated senescent cells (Fig. 4). The second pattern is currently under investigation in our laboratory. Finally, because PPARγ levels remained constant during successive passages (Fig. 7), we hypothesize that the third mechanism is not involved in PPAR-regulated senescence in 2BS and WI-38 cells.

$p16^{INK4\alpha}$ is an important cell-cycle inhibitor that can induce senescence and repress tumor cell growth (Collins and Sedivy, 2003). Its loss or inactivation is correlated with cell immortality

(Ruas and Peters, 1998). Although $p16^{INK4\alpha}$ plays an important role in cellular senescence and tumorigenesis, its transcriptional control is poorly understood. Here, we report, for the first time to our knowledge, the molecular mechanism by which PPARγ upregulates the expression of $p16^{INK4\alpha}$ in 2BS and WI-38 cells. Our results, which show that $p16^{INK4\alpha}$ is required for PPARγ-agonist-induced senescence (Fig. 6), verify this assertion. However, recent studies have proposed p16 regulatory pathways that are distinct from those described here. Ohtani et al. proposed a model in which the upregulation of $p16^{INK4\alpha}$ depended on the accumulation of Ets1 and the absence of interference by Id1 during senescence (Ohtani et al., 2001). Zheng et al. found that Id1 regulated $p16^{INK4\alpha}$ levels through interactions with E47 (Zheng et al., 2004). Wang et al. reported that a 24-kDa protein might inhibit the expression of $p16^{INK4\alpha}$ by interacting with the INK4α transcription silence element (ITSE) (Wang et al., 2001). These findings do not contradict the present conclusions. It is clear that the *p16* promoter is subject to multiple levels of control (Hara et al., 1996; Jacobs et al., 1999); therefore, p16 regulation cannot be explained by a single isolated pathway.

In summary, in senescent cells, dephosphorylation of PPARγ increases its transcriptional activity. The increased PPARγ activity might be one reason for the elevated $p16^{INK4\alpha}$ expression in senescent 2BS and WI-38 cells, which in turn contributes to the onset of cellular senescence (Fig. 9). Various polyunsaturated fatty acids, the major dietary constituents, are specific ligands for PPARγ (Forman et al., 1995; Kahn et al., 2000). Much research shows that fatty acids can influence the transcriptional activity of PPARγ. In our study, PPARγ accelerated senescence by inducing $p16^{INK4\alpha}$ expression in a ligand-dependent manner; therefore, PPARγ might underlie a key switch between exterior factors (such as diet) and interior factors (such as the *p16* gene). Finally, we demonstrated a gene-environment effect induced by PPARγ-agonist administration, which results in senescence-like growth arrest with $p16^{INK4\alpha}$ expression. The effect was more marked in senescent cells than in young cells. Our study might offer an opportunity to investigate gene-environment interactions associated with cellular senescence in health and disease.

Materials and Methods

Antibodies, reagents and plasmids

Antibodies against PPARγ (SC-7273), PPARα (SC-9000), PPARβ (SC-1983) and β-actin (SC-1616) were purchased from Santa Cruz Biotechnology. Anti-phospho-PPARγ (05-816) and anti-p16 (MS-887-P1) antibodies were purchased from Upstate. Pioglitazone and GW9662 were purchased from Cayman. Troglitazone was purchased from Calbiochem or Cayman. The PPARγ expression plasmid cloned in pcDNA3.1 was constructed as described previously (Fu et al., 2001). *p16* cDNA in pBluescript was a kind gift from David Beach (Howard Hughes Medical Institute, Cold Spring Harbor, NY). The full-length *p16* cDNA (800 bp) was placed into the expression vector pcDNA3.1 in both orientations. A *p16*-promoter fragment that contained 1040 bp was obtained via PCR from the 3070-bp pGL2-Basic vector, which was generously provided by Gorden Peters (Imperial Cancer Research Fund Laboratories, London, UK).

siRNA preparation

The siRNA was designed as reported previously. The sequence of the sense strand of *PPARγ* siRNA was 5′-GCCCTTCACTACTGTTGAC-3′ (Kelly et al., 2004); *p16* siRNA was 5′-AGAACCAGAGAGGCTCTGA-3′ (Zhou et al., 2004); and negative control siRNA was 5′-TTCTCCGAACGTGTCACGT-3′ (Genechem). The hairpin-siRNA template oligonucleotides were chemically synthesized with 5′-phosphate, 3′-hydroxyl, and two base overhangs on each strand. Then the template oligonucleotides were inserted into the *Bam*HI and *Hin*dIII sites of the pSilencer 2.1-U6 neo vector.

Cell culture and transfection

Human embryonic lung diploid fibroblast 2BS cells (obtained from the National Institute of Biological Products, Beijing, China) were previously isolated from female fetal lung fibroblast tissue and have been fully characterized (Tang et al., 1994). The current expected lifespan is approximately PD70. 2BS cells are considered to be young at PD30 or below and to be fully senescent at PD55 or above. Human embryonic lung diploid fibroblast WI-38 cells (ATCC number: CCL75) were obtained from the Chinese Academy of Sciences (Shanghai, China). The current expected lifespan is approximately PD55. WI-38 cells are considered to be young at PD25 or below and to be fully senescent at PD50 or above. Cells were maintained in Dulbecco's modified Eagle's medium (Gibco) supplemented with 10% fetal bovine serum (FBS, Hyclone), 100 units/ml penicillin, and 100 μg/ml streptomycin at 37°C in 5% CO_2.

Young cells were grown to 80-90% confluence. Expression plasmids were transfected with Lipofectin reagent (Life Technologies) according to the manufacturer's instructions. Pools of stable transformants were obtained by sustained selection of 300 μg/ml G418 (Life Technologies). PDs were calculated with the formula PD=log(*n*2/*n*1)/log2, where *n*1 is the number of cells seeded and *n*2 is the number of cells recovered (Shay and Wright, 1989).

Growth curves

Cells were detached and seeded into 96-well plates, with 2000 cells per well. After overnight incubation, cells were treated with 20 μM troglitazone or 10 μM pioglitazone diluted in DMSO (Sigma). All cells received identical volumes of DMSO and were exposed to each drug for 6 days; medium and drug were changed every 48 hours. At the indicated times, cells were stained with 20 μl 3-(4, 5-dimethylthiazol-2-yl)-2, 5-diphenyltetrazolium bromide (MTT, 10 mg/ml in PBS; Sigma) for 3 hours and then dissolved with DMSO. The optical density at 570 nm was determined.

Cell-cycle analysis and synchronization

When cells reached 70-80% confluence, they were washed with PBS, detached with 0.25% trypsin and fixed with 75% ethanol overnight. After treatment with 1 mg/ml RNase A (Sigma) at 37°C for 30 minutes, cells were resuspended in 0.5 ml of PBS and stained with propidium iodide in the dark for 30 minutes; DNA contents were measured by fluorescence-activated cell sorting on a FACScan flow cytometry system (BD Biosciences). The data were analyzed using CellFiT software.

For synchronization, 2BS cells were rendered quiescent by serum deprivation for 48 hours and then stimulated to re-enter the cell cycle by the addition of serum to a final concentration of 10%. G1-phase cells were harvested at 8 hours after serum stimulation.

SA-β-gal staining

Cells were washed twice in PBS, fixed for 3-5 minutes at room temperature in 3% formaldehyde and washed with PBS again. Then cells were incubated overnight at 37°C without CO_2 in a freshly prepared staining solution [1 mg/ml 5-bromo-4-chloro-3-indolyl-β-D-galactopyranoside (X-gal), 40 mM citric acid/sodium phosphate, pH 6.0, 5 mM potassium ferrocyanide, 5 mM potassium ferricyanide, 150 mM NaCl, 2 mM $MgCl_2$] (Dimri et al., 1995). At least 200 cells were counted in randomly chosen fields from each culture well.

Western blotting

Cells were lysed in modified radioimmune precipitation assay (RIPA) buffer (50 mM Tris-HCl, pH 7.4, 150 mM NaCl, 1 mM EDTA, 0.25% Na-deoxycholate, 1% NP-40, 10 μg/ml aprotinin, 10 μg/ml leupeptin, 1 mM phenylmethylsulfonyl fluoride, 0.2 mM sodium orthovanadate, 1 mM NaF). Protein concentration of each sample was determined by BCA protein assay reagent (Pierce); 100-150 μg of protein was electrophoresed on 15% SDS-polyacrylamide gel and transferred to nitrocellulose membrane (Millipore). The membrane was blocked and then incubated with the primary antibody in 5% non-fat dry milk in TBST (10 mM Tris-Cl, pH 7.5, 150 mM NaCl, 0.05% Tween 20) overnight at 4°C. After washing, the blots were incubated with secondary antibody conjugated to horseradish peroxidase (Amersham Biosciences) at 1:40,000 in TBST for 1 hour at room temperature. Proteins were visualized with Chemiluminescent Substrate (Pierce) according to manufacturer's instructions.

Site-directed mutagenesis

Substitution mutations were generated using the QuikChange mutagenesis kit (Stratagene) according to the manufacturer's instructions. Synthetic oligonucleotides that contained the desired bases were used in the mutagenesis. The sequence of mutations for nucleotides at positions –1023 and –1022 (GG-CC) of the 5′-flanking region of the *p16* promoter was 5′-GTGTGAACCAGACAGGACAGTATTT-3′ (GG-CC mutation underlined) (Gizard et al., 2005); mutant PPARγ with the substitution of serine-84 to alanine was 5′-GTGGAGCCTGCAGCTCCACCTTATTATTC-3′ (TCT-GCT mutation) (Adams et al., 1997). DNA that incorporated the desired mutations was transformed into XL1-Blue supercompetent cells. Plasmid DNA was prepared and the presence of the mutations was confirmed by sequencing.

Chromatin immunoprecipitation

ChIPs were performed using the Chromatin Immunoprecipitation Assay kit (Upstate) according to manufacturer's instructions. For each experimental condition, 1×10^6 cells were used. At 48 hours before harvesting, cells were pre-treated with 20 μM troglitazone, 10 μM pioglitazone, 10 μM GW9662, or 1% DMSO (vehicle) as control.

Cells were sonicated and lysates immunoprecipitated using the indicated antibodies. To amplify PPRE regions of the *p16* promoter, the following sequences of the primers were used: p16 PPREs, 5′-GCACTCATATTCCCTTCCCCCCT-3′; p16 PPREa, 5′-GGAAGGACGGACTCCATTCTCAAAG-3′. Control p16 element was located immediately downstream of PPRE. The sequences of the primers used were as follows: p16 controls, 5′-GAAGCTGGTCTTTGGATCACTGTGC-3′; p16 controla, 5′-GACGGGGGAGAATTCTGCCTGT-3′ (Gizard et al., 2005). All primers were synthesized at Sunbio Biotechnology (Beijing, China).

Real-time PCR and data analysis

Two-step real-time PCR was performed with 5 μl of DNA and 400 nM primers diluted to a final volume of 50 μl in SYBR Green Master Mix (Applied Biosystems). Accumulation of fluorescent products was monitored by real-time PCR using an Applied Biosystem 7300 real-time PCR system (Applied Biosystems). A melting curve was generated to ensure that a single peak of the predicted Tm was produced and no primer-dimer complexes were present. Single amplicon generation was verified by agarose gel electrophoresis. No PCR products were observed in the absence of template. Sequence Detector software (version 1.3.1) was used for data analysis and relative fold induction was determined by the comparative threshold cycle (CT). Fold-enrichments were determined by the method described in the Applied Biosystems User Bulletin and data analysis followed the methodology described in a recent report (Frank et al., 2001). Fold differences were calculated by correcting for each signal concentration with the concentration of input signal for each sample [(signal concentration)/(input concentration)]. Real-time RT-PCR data figures were generated using Microsoft Excel (Microsoft Corporation, USA).

Luciferase assay

2BS cells were plated in six-well culture plates in triplicate for each condition at an initial concentration of 2×10^5 cells/well. pGL2 luciferase reporter constructs driven by the indicated 1 μg p16 wild-type (p16 WT) or mutant (p16 mutant) promoter fragments were co-transfected with 3 μg pcDNA3.1 (vector), wild-type pcDNA-PPARγ (PPARγ or WT), mutant pcDNA-PPARγ (S84A), pSilencer 2.1-U6 neo (RNAi vector) or pSilencer-PPARγ (siPPARγ) expression plasmid. The amount of plasmid in the transfection mixture was equalized to 4 μg by adding pcDNA3.1 vector. *Renilla* luciferase reporter plasmid pRL-CMV (10 ng) was also co-transfected into each well as an internal control. After 24 hours, cells were treated with 20 μM troglitazone, 10 μM pioglitazone or 10 μM GW9662. Luciferase activity was assessed with a dual-luciferase reporter assay system (Promega) according to manufacturer's instructions after 48 hours of drug treatment. The enzyme activity was normalized for efficiency of transfection on the basis of *Renilla* luciferase activity levels and reported as relative light units (RLU). All reporter assays were performed in triplicate on at least two individual experiments and standard errors are denoted by bars in the figures.

Reverse-transcription PCR

Total RNA was isolated from 2BS cells by RNeasy kit (QIAGEN). After denaturing the total RNA at 70°C for 10 minutes, cDNA was synthesized with oligo-dT primer and reverse transcriptase (Invitrogen). PCR amplification was performed using specific primers for PPARγ as follows: PPARγs, 5′-GAGCCCAAGTTTGAGTTTGC-3′; PPARγa, 5′-TGGAAGAAGGGAAATGTTGG-3′. The sequences of the primers used for p16 were: p16s, 5′-CCCAACGCACCGAATAGT-3′; p16a, 5′-ATCTAAGT-TTCCCGAGGTT-3′. The sequences of the primers used for GAPDH were: GAPDHs, 5′-CGAGTCAACGGATTTGGTGGTAT-3′; GAPDHa, 5′-AGCCTTCTCCATGG-TGAAGAC-3′. PCR products were loaded onto an agarose gel and stained with ethidium bromide.

Statistical analysis

The data are reported as mean ± s.d. of the indicated number of experiments. Values were assessed by pairwise (one-way analysis of variance, ANOVA). In all cases, $P\leqslant0.05$ and $P\leqslant0.01$ was considered significant.

We thank Wengong Wang for helpful discussions. This work was supported by grants from the National Basic Research Programs of China (No. 2007CB507400) and the National Natural Science Foundation of China (No. 30671064).

References

Adams, M., Reginato, M. J., Shao, D., Lazar, M. A. and Chatterjee, V. K. (1997). Transcriptional activation by peroxisome proliferator-activated receptor γ is inhibited by phosphorylation at a consensus mitogen-activated protein kinase site. *J. Biol. Chem.* **272**, 5128-5132.

Bendixen, A. C., Shevde, N. K., Dienger, K. M., Willsondagger, T. M., FunkDagger, C. D. and Pike, J. W. (2001). IL-4 inhibits osteoclast formation through a direct action on osteoclast precursors via peroxisome proliferator-activated receptor gamma 1. *Proc. Natl. Acad. Sci. USA* **98**, 2443-2448.

Campisi, J. (2001). Cellular senescence as a tumor-suppressor mechanism. *Trends Cell Biol.* **11**, S27-S31.

Campisi, J. (2005). Suppressing cancer: the importance of being senescent. *Science* **309**, 886-887.

Chang, T. H. and Szabo, E. (2000). Induction of differentiation and apoptosis by ligands of peroxisome proliferator-activated receptor gamma in non-small cell lung cancer. *Cancer Res.* **60**, 1129-1138.

Collins, C. J. and Sedivy, J. M. (2003). Involvement of the INK4a/Arf gene locus in senescence. *Aging Cell* **2**, 145-150.

Dai, C. Y. and Enders, G. H. (2000). p16 INK4a can initiate an autonomous senescence program. *Oncogene* **19**, 1613-1622.

Dimri, G. P., Lee, X., Basile, G., Acosta, M., Scott, G., Roskelley, C., Medrano, E. E., Linskens, M., Rubelj, I. and Pereira-Smith, O. (1995). A biomarker that identifies senescent human cells in culture and in aging skin in vivo. *Proc. Natl. Acad. Sci. USA* **92**, 9363-9367.

Duan, J., Zhang, Z. and Tong, T. (2001). Senescence delay of human diploid fibroblast induced by anti-sense $p16^{INK4a}$ expression. *J. Biol. Chem.* **276**, 48325-48331.

Elstner, E., Muller, C., Koshizuka, K., Williamson, E. A., Park, D., Asou, H., Shintaku, P., Said, J. W., Heber, D. and Koeffler, H. P. (1998). Ligands for peroxisome proliferator-activated receptorgamma and retinoic acid receptor inhibit growth and induce apoptosis of human breast cancer cells in vitro and in BNX mice. *Proc. Natl. Acad. Sci. USA* **95**, 8806-8811.

Forman, B. M., Tontonoz, P., Chen, J., Brun, R. P., Spiegelman, B. M. and Evans, R. M. (1995). 15-Deoxy-delta **12**, 14-prostaglandin J2 is a ligand for the adipocyte determination factor PPAR gamma. *Cell* **83**, 803-812.

Frank, S. R., Schroeder, M., Fernandez, P., Taubert, S. and Amati, B. (2001). Binding of c-Myc to chromatin mediates mitogen-induced acetylation of histone H4 and gene activation. *Genes Dev.* **15**, 2069-2082.

Fu, M., Zhang, J., Zhu, X., Myles, D. E., Willson, T. M., Liu, X. and Chen, Y. E. (2001). Peroxisome proliferator-activated receptor gamma inhibits transforming growth factor beta-induced connective tissue growth factor expression in human aortic smooth muscle cells by interfering with Smad3. *J. Biol. Chem.* **276**, 45888-45894.

Gizard, F., Amant, C., Barbier, O., Bellosta, S., Robillard, R., Percevault, F., Sevestre, H., Krimpenfort, P., Corsini, A., Rochette, J. et al. (2005). PPAR alpha inhibits vascular smooth muscle cell proliferation underlying intimal hyperplasia by inducing the tumor suppressor p16INK4a. *J. Clin. Invest.* **115**, 3228-3238.

Goldstein, S. (1990). Replicative senescence: the human fibroblast comes of age. *Science* **249**, 1129-1133.

Guan, Y. F., Zhang, Y. H., Breyer, R. M., Davis, L. and Breyer, M. D. (1999). Expression of peroxisome proliferator-activated receptor gamma (PPARgamma) in human transitional bladder cancer and its role in inducing cell death. *Neoplasia* **1**, 330-339.

Han, J., Hajjar, D. P., Tauras, J. M., Feng, J., Gotto, A. M., Jr and Nicholson, A. C. (2000). Transforming growth factor-beta1 (TGF-beta1) and TGF-beta2 decrease expression of CD36, the type B scavenger receptor, through mitogen-activated protein kinase phosphorylation of peroxisome proliferator-activated receptor-gamma. *J. Biol. Chem.* **275**, 1241-1246.

Hara, E., Smith, R., Parry, D., Tahara, H., Stone, S. and Peters, G. (1996). Regulation of p16CDKN2 expresstion and its implications for cell immortalization and senescence. *Mol. Cell. Biol.* **16**, 859-867.

Hayflick, L. (1965). The limited in vitro lifetime of human diploid cell strains. *Exp. Cell Res.* **37**, 614-636.

Hayflick, L. and Moorhead, P. S. (1961). The serial cultivation of human diploid cell strains. *Exp. Cell Res.* **25**, 585-621.

Hu, E., Kim, J. B., Sarraf, P. and Spiegelman, B. M. (1996). Inhibition of adipogenesis through MAP kinase-mediated phosphorylation of PPARgamma. *Science* **274**, 2100-2103.

Jacobs, J. J. L., Kieboom, K., Marino, S., DePinho, R. A. and van Lohuizen, M. (1999). The oncogene and Polycomb-group gene bmi-1 regulates cell proliferation and senescence through the ink4a locus. *Nature* **397**, 164-168.

Johnson, K. D. and Bresnick, E. H. (2002). Dissecting long-range transcriptional mechanisms by chromatin immunoprecipitation. *Methods* **26**, 27-36.

Kahn, C. R., Chen, L. and Cohen, S. E. (2000). Unraveling the mechanism of action of thiazolidinediones. *J. Clin. Invest.* **106**, 1305-1307.

Kelly, D., Campbell, J. I., King, T. P., Grant, G., Jansson, E. A., Coutts, A. G., Pettersson, S. and Conway, S. (2004). Commensal anaerobic gut bacteria attenuate inflammation by regulating nuclear-cytoplasmic shuttling of PPAR-gamma and RelA. *Nat. Immunol.* **5**, 104-112.

Kirkland, J. L., Tchkonia, T., Pirtskhalava, T., Han, J. and Karagiannides, I. (2002). Adipogenesis and aging: does aging make fat go MAD? *Exp. Gerontol.* **37**, 757-767.

Krishnamurthy, J., Torrice, C., Ramsey, M. R., Kovalev, G. I., Al-Regaiey, K., Su, L. and Sharpless, N. E. (2004). Ink4a/Arf expression is a biomarker of aging. *J. Clin. Invest.* **114**, 1299-1307.

Kubota, T., Koshizuka, K., Koike, M., Uskokovic, M., Miyoshi, I. and Koeffler, H. P. (1998). 19-nor-26,27-bishomo-vitamin D3 analogs: a unique class of potent inhibitors of proliferation of prostate, breast, and hematopoietic cancer cells. *Cancer Res.* **58**, 3370-3375.

Lazennec, G., Canaple, L., Saugy, D. and Wahli, W. (2000). Activation of peroxisome proliferator-activated receptors (PPARs) by their ligands and protein kinase A activators. *Mol. Endocrinol.* **14**, 1962-1975.

Mangelsdorf, D. J., Thummel, C., Beato, M., Herrlich, P., Schutz, G., Umesono, K., Blumberg, B., Kastner, P., Mark, M., Chambon, P. et al. (1995). The nuclear receptor superfamily: the second decade. *Cell* **83**, 835-839.

Michalik, L., Desvergne, B. and Wahli, W. (2004). Peroxisome-proliferator-activated receptors and cancers: complex stories. *Nat. Rev. Cancer* **4**, 61-70.

Moerman, E. J., Teng, K., Lipschitz, D. A. and Lecka-Czernik, B. (2004). Aging activates adipogenic and suppresses osteogenic programs in mesenchymal marrow stroma/stem

cells: the role of PPAR-gamma2 transcription factor and TGF-beta/BMP signaling pathways. *Aging Cell* **3**, 379-389.

Mueller, E., Sarraf, P., Tontonoz, P., Evans, R. M., Martin, K. J., Zhang, M., Fletcher, C., Singer, S. and Spiegelman, B. M. (1998). Terminal differentiation of human breast cancer through PPAR gamma. *Mol. Cell* **1**, 465-470.

Ohtani, N., Zebedee, Z., Huot, T. J. G., Stinson, J. A., Sugimoto, M., Ohashi, Y., Sharrocks, A. D. and Peters, G. (2001). Opposing effects of Ets and Id proteins on p16INK4a expression during cellular senescence. *Nature* **409**, 1067-1070.

Picard, F., Kurtev, M., Chung, N., Topark-Ngarm, A., Senawong, T., Machado De Oliveira, R., Leid, M., McBurney, M. W. and Guarente, L. (2004). Sirt1 promotes fat mobilization in white adipocytes by repressing PPAR-gamma. *Nature* **429**, 771-776.

Ruas, M. and Peters, G. (1998). The p16INK4a/CDKN2A tumor suppressor and its relatives. *Biochim. Biophys. Acta* **1378**, F115-F177.

Sarraf, P., Mueller, E., Jones, D., King, F. J., DeAngelo, D. J., Partridge, J. B., Holden, S. A., Chen, L. B., Singer, S., Fletcher, C. et al. (1998). Differentiation and reversal of malignant changes in colon cancer through PPARgamma. *Nat. Med.* **4**, 1046-1052.

Sasaki, H., Tanahashi, M., Yukiue, H., Moiriyama, S., Kobayashi, Y., Nakashima, Y., Kaji, M., Kiriyama, M., Fukai, I., Yamakawa, Y. et al. (2002). Decreased perioxisome proliferator-activated receptor gamma gene expression was correlated with poor prognosis in patients with lung cancer. *Lung Cancer* **36**, 71-76.

Shay, J. W. and Wright, W. E. (1989). Quantitation of the frequency of immortalization of normal human diploid fibroblasts by SV40 large T-antigen. *Exp. Cell Res.* **184**, 109-118.

Tang, Z., Zhang, Z., Zheng, Y., Corbley, M. J. and Tong, T. (1994). Cell aging of human diploid fibroblasts is associated with changes in responsiveness to epidermal growth factor and changes in HER-2 expression. *Mech. Ageing Dev.* **73**, 57-67.

Tontonoz, P., Singer, S., Forman, B. M., Sarraf, P., Fletcher, J. A., Fletcher, C. D., Brun, R. P., Mueller, E., Altiok, S., Oppenheim, H. et al. (1997). Terminal differentiation of human liposarcoma cells induced by ligands for peroxisome proliferator-activated receptor gamma and the retinoid X receptor. *Proc. Natl. Acad. Sci. USA* **94**, 237-241.

Wang, W., Wu, J., Zhang, Z. and Tong, T. (2001). Characterization of regulatory elements on the promoter region of p16(INK4a) that contribute to overexpression of p16 in senescent fibroblasts. *J. Biol. Chem.* **276**, 48655-48661.

Weinstein, B. S. and Ciszek, D. (2002). The reserve-capacity hypothesis: evolutionary origins and modern implications of the trade-off between tumor-suppression and tissue-repair. *Exp. Gerontol.* **37**, 615-627.

Willson, T. M., Cobb, J. E., Cowan, D. J., Wiethe, R. W., Correa, I. D., Prakash, S. R., Beck, K. D., Moore, L. B., Kliewer, S. A. and Lehmann, J. M. (1996). The structure-activity relationship between peroxisome proliferator-activated receptor gamma agonism and the antihyperglycemic activity of thiazolidinediones. *J. Med. Chem.* **39**, 665-668.

Wong, H. and Riabowol, K. (1996). Differential CDK-inhibitor gene expression in aging human diploid fibroblasts. *Exp. Gerontol*. **31**, 311-325.

Wright, H. M., Clish, C. B. and Spiegelman, B. M. (2000). A synthetic antagonist for the peroxisome proliferator-activated gamma ligand inhibits adipocyte differentiation. *J. Biol. Chem.* **275**, 1873-1877.

Ye, P., Zhang, X. J., Wang, Z. J. and Zhang, C. (2006). Effect of aging on the expression of peroxisome proliferator-activated receptor gamma and the possible relation to insulin resistance. *Gerontology* **52**, 69-75.

Zheng, W., Wang, H., Xue, L., Zhang, Z. and Tong, T. (2004). Regulation of cellular senescence and p16(INK4a) expression by Id1 and E47 proteins in human diploid fibroblast. *J. Biol. Chem.* **279**, 31524-31532.

Zhou, H. W., Lou, S. Q. and Zhang, K. (2004). Recovery of function in osteoarthritic chondrocytes induced by p16INK4a-specific siRNA in vitro. *Rheumatology Oxford* **43**, 555-568.

Journal of Cell Science